

New Development of Hexahedral Type Vibration Motor Used for Mobile Phones

Gun-Yong Hwang, Sang-Moon Hwang*, Shi-Uk Chung

School of Mechanical Engineering, Pusan National University, Pusan 609-735, Korea

Beom-Soo Kang

Department of Aerospace Engineering, Pusan National University, Pusan 609-735, Korea

I-Cheol Hwang

*Division of Mechanical and Industrial System Engineering, Dong-eui University,
Pusan 614-714, Korea*

Mobile communication industry powered by electronics and information technology is building a transforming way for human communication. The latest electronics is so saturated to forget the difficulty in size reduction of electronic parts. However, mechanical parts, such as dynamic speakers and vibration motors, are intrinsically not easy to realize size reduction due to their construction. In this paper, a hexahedral type with simpler configuration is introduced to substitute for the conventional vibration motors. For uneven magnetic field analysis of the hexahedral type, FEM was used to determine magnetic flux density. After an analysis of magnetic and mechanical characteristics, it is shown that the coil configuration is the most important parameter to increase the output torque, and thus vibration. For optimization, genetic algorithm is used to find the optimal configuration of coil to maximize the output torque. Experimental results are also followed to confirm the validity of the proposed design.

Key Words : Hexahedral Type Vibration Motor, FEM, Genetic Algorithm

1. Introduction

The wide use of mobile phones has revolutionized human communication. However, paging sound from mobile phones often acts as one of environmental noise sources these days. Silent tactile signal by vibration motor is preferred to sound signal in many occasions. Driven by the increased customers demands, most mobile phones of today meet the various functional and performance requirements without difficulty. For mechanical parts, such as dynamic speakers and

vibration motors, the performance heavily depends on size and weight. Noting that these devices are to be carried by users, size and weight becomes important measure for the value of the devices. This paper presents a new hexahedral type vibration motor which has great advantages over the conventional ones in mounting and transmission of vibration due to its unique shape.

A lot of research has been done to calculate flux linkage, back-EMF and output torque for PM(permanent magnet) motors with circular cross section (Jang and Lieu, 1996; Alhamadi and Demerdash, 1994; Liu, et al, 1994). For the motors with square cross section that is to be presented in this paper, however, analysis of the magnetic field and the output torque has yet to be found.

In this paper, FEM is used to determine magnetic field distribution of a coreless hexahedral

* Corresponding Author,

E-mail : shwang@hyowon.ac.kr

TEL : +82-51-510-3204; FAX : +82-51-514-7640

School of Mechanical Engineering, Pusan National University, Pusan 609-735, Korea. (Manuscript Received October 10, 2001; Revised May 8, 2002)

Table 1 Characteristic features of vibration motors

	Coin type	Cylinder type	Hexahedral type
Winding	Coreless winding	Rhombic winding	Coreless winding
Airgap	Axial gap	Radial gap	Radial gap
Coil type	Embedded in the rotor	Moving coil	Attached to the rotor
Eccentric rotor	Internal eccentric rotor	External eccentric rotor	Internal eccentric rotor
Connection	WYE	DELTA	WYE

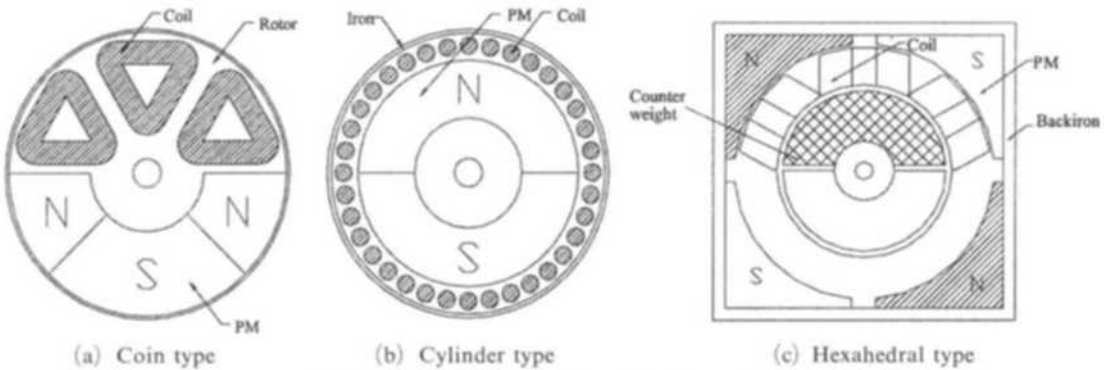


Fig. 1 Schematics of various vibration motors

type vibration motor with non-circular shaped PM. To maximize the output torque and vibration quantity, genetic algorithm is used as an optimization tool. Figure 1 shows two types of conventional vibration motors that are presently commercialized, a coin type and a cylinder type, and a simpler hexahedral type that is introduced in this paper and Table 1 lists characteristic features of them.

2. Method of Analysis

Magnetic field distribution of a PM DC motor can be determined by solving the governing equation, as in Eq. (1) with appropriate boundary conditions. To consider non-circular shaped PM, commercial FEM solver, ANSYS, is used to find magnetic field density.

$$\frac{\partial^2 \Psi_I}{\partial r^2} + \frac{1}{r} \frac{\partial \Psi_I}{\partial r} + \frac{1}{r^2} \frac{\partial^2 \Psi_I}{\partial \theta^2} = 0; \text{ in airspace}$$

$$\frac{\partial^2 \Psi_{II}}{\partial r^2} + \frac{1}{r} \frac{\partial \Psi_{II}}{\partial r} + \frac{1}{r^2} \frac{\partial^2 \Psi_{II}}{\partial \theta^2} = \frac{M_r}{r\mu_r}; \text{ in PM (1)}$$

where Ψ , μ_r , M_r are magnetic scalar potential, relative permeability of PM and radial compo-

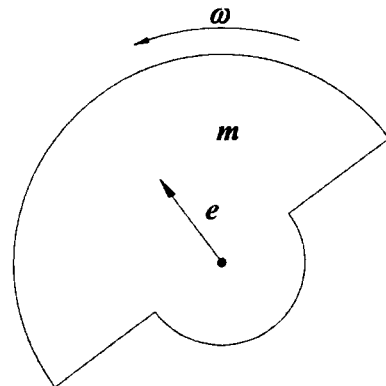


Fig. 2 Eccentric rotor

nent of magnetization vector respectively. The exciting force by an eccentric rotor as shown in Fig. 2 can be expressed as;

$$F = me\omega^2 \tag{2}$$

where m , e , ω are rotor mass, rotor eccentricity and rotating speed respectively. It can be seen that ω is the most important factor since the exciting force is proportional to the square of it. The rotating speed of a motor can be determined by the dynamic equation of the motor as in Eq. (3).

$$T = J \frac{d\omega}{dt} + D \cdot \omega + T_f \quad (3)$$

where T , J , D and T_f denote output torque, moment of inertia, damping coefficient and friction torque respectively. For a steady state operation in which the rotating speed is constant, the rotating speed can be expressed as;

$$\omega_{s.s} = \frac{T - T_f}{D} \quad (4)$$

Noting that T_f and D are governed by mechanical design of the given motor, T is the only electromagnetic design parameter to increase the exciting force, and can be written as;

$$T = \frac{\sum e_j \cdot i_j}{\omega} \quad (5)$$

where e_j is the phase back-EMF and i_j is the phase current.

The back-EMF, defined as the time rate change of the flux linkage can be expressed as in Eq. (6). The phase current can be obtained by solving the voltage equation as in Eq. (7). Noting that the phase current is almost constant in a coreless motor due to negligible phase inductance, back-EMF constant is to be maximized to maximize the output torque, and thus the resultant vibration.

$$e_j = \frac{d\lambda_j}{dt} = \frac{d(N\Phi_j(\theta))}{d\theta} \cdot \frac{d\theta}{dt} \quad (6)$$

$$V = i_j R + L \frac{di_j}{dt} + e_j \quad (7)$$

where λ_j , N , Φ_j , θ , V , R and L denote flux linkage per coil, number of turns per coil, total flux per coil, rotor position angle, applied voltage, coil resistance and inductance respectively.

3. Results on Magnetics

For the prototype hexahedral vibration motor as shown in Fig. 1, Fig. 3 shows radial flux density distribution along the several radii contours, showing a dramatic change near the PM region. Figure 4 shows configuration of coil topology to be used, where α_1 , β_2 , l and n denote coil inner arc angle, coil outer arc angle, number of turns aligned in tangential direction and num-

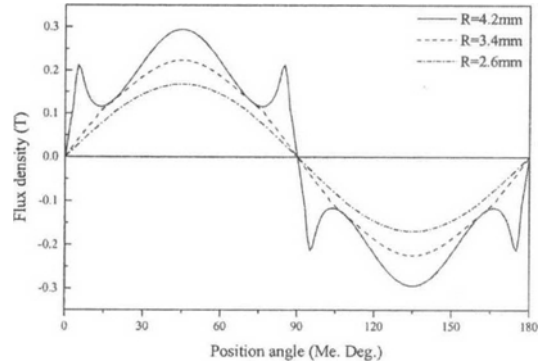


Fig. 3 Flux density distribution calculated by FEM

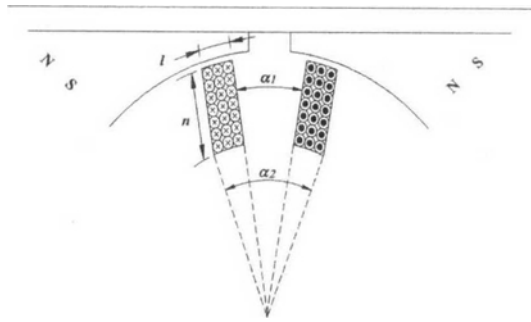


Fig. 4 Configuration of coil topology

ber of turns aligned in radial direction respectively. To obtain the output torque by single coil with unit current input for various coil configurations, a matrix of discrete radial flux density is prepared with a resolution of 0.5° in tangential direction and 0.05mm in radial direction which corresponds to coil diameter as shown in Eq. (8). With the matrix, the output torque by single coil with unit current input can be expressed as in Eq. (9).

$$B_r(r_j, \theta_j) = \begin{bmatrix} B_r(r_1, \theta_1) & \cdots & B_r(r_1, \theta_l) \\ \cdots & \cdots & \cdots \\ B_r(r_n, \theta_1) & \cdots & B_r(r_n, \theta_l) \end{bmatrix} \quad (8)$$

$$T = \frac{d}{d\theta} \left[N \sum_{i=1}^n \sum_{j=1}^l B_r(r_i, \theta_j) A_{ij} \right] \quad (9)$$

where B_r , r_i and A_{ij} denote flux density, radii to coil and corresponding areas for the flux linkage. Using the proposed method, only single FEM analysis is required for the radial magnetic field distribution and can be also used as an objective function for optimization. To ensure the validity

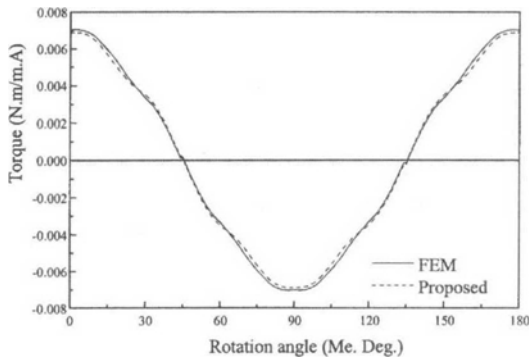


Fig. 5 Torque waveform by single coil with unit current input

of the proposed method, Fig. 5 shows comparison of output torque between the proposed method and purely FEM with unit current input, and shows a good agreement.

4. Optimization by Genetic Algorithm

In the early 1970s, Holland proposed genetic algorithm (GA) as a computer program that emulates the evolutionary process of nature to find out the global optimal solution. GA has been successfully applied to optimization problems in many fields. They can find the global optimal solution, and also handle directly discrete parameters. In a genetic code, some operators similar to those of natural genetics are used. The three manipulated operators are encoded strings of bits from a binary code, and affect the make-up of a chromosome based on biologically inspired-selection, crossover and mutation (Wurtz et al., 1997).

In optimization process of the given motor, fitness values are assigned to each other according to the magnitude of T_{rms} . In other words, high fitness values are to be assigned for the higher torque value, and the lower one, otherwise. If the ratio of high and low fitness values is too low, GA will make quite long generations with fear of convergence to the local minimum. This algorithm uses the exponent of T_{rms} to assign high fitness value to the higher T_{rms} for the fast convergence.

As for the parameter constraints, a_2 is set to be

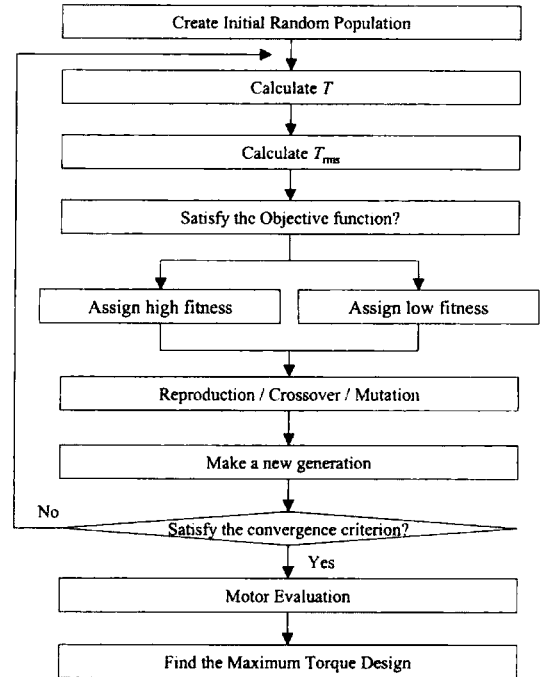


Fig. 6 Flow chart of genetic algorithm

60° for the maximum use of the space, and l is also limited by the number of axial stacks by 25. To maintain the same coil resistance, thus the same input power, n is also determined by fixing the total number of turns. To ensure the fast convergence to the optimal solution, weighting factor is used in fitness function as shown in Eq. (10).

$$F_{fit} = \exp(C_{fit} \times T_{rms}) \quad (10)$$

where C_{fit} which depends on T_{rms} value is defined as the fitness constant given by the user. It controls the increment of objective function. It also changes position of search field range, and leads more powerful convergence and more reasonable results. Figure 6 shows the overall flow chart of genetic algorithm. Optimized design parameters and T_{rms} are presented in Table 2 and compared with prototypes. Figure 7 shows the corresponding output torque waveform by single coil with unit current input. T_{rms} is 12% higher than that of prototype 1 and 21% higher than that of prototype 2 after optimization by GA with a little modification of coil geometry and without change in overall size and weight.

Table 2 Motor design parameters for the analysis

Parameters	Unit	Prototype 1	Prototype 2	Optimized model
α_1	Degree	14°	20°	24.1°
l	—	25	16	20
N	—	16	25	20
T_{rms}	N·m/m·A	0.002034	0.001823	0.002314

Table 3 Comparison of specifications

	Coin type	Cylinder type	Hexahedral type
Size (mm)	$\phi 14 \times t 3.8$	$10 \times 10 \times t 4.0$	$\phi 4 \times l 20$
Volume (mm ³)	585	400	250
Weight (g)	2.5	1.8	1.4
Current (mA)	30	40	40
Voltage (V)	3.0	3.0	2.3

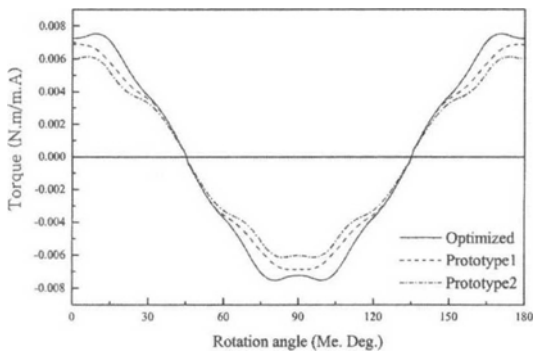


Fig. 7 Comparison of output torque between prototypes and optimized model

5. Vibration Quantity Evaluation Test

Acceleration by vibration motors is the most common parameter to define vibration quantity. However, it is obvious that the acceleration measured at a certain point depends on mounting points and postures as well. For overall comparison of three types, various motor mounting points and acceleration measuring points are chosen in performance evaluation. The mounting points and the measuring points are marked on the test dummy block of Al (100mm × 40mm × 20mm) as shown in Fig. 8, where A and B indicate accelerometer mounting points, and 1~4 indicate the vibration motor mounting points. All conven-

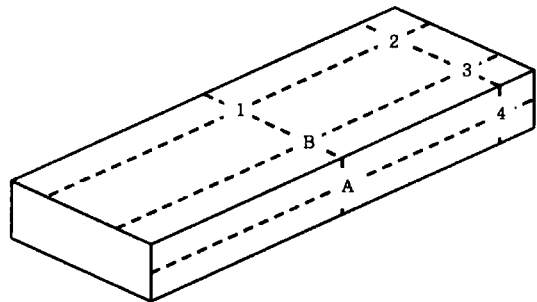


Fig. 8 Mounting points on dummy block

tional vibration motors can be mounted at points 1, 2 and 3, but point 4 is available only for the cylinder type and the hexahedral type while the coin type is difficult to be mounted due to the size.

For the measurement of vibration quantity, a test setup is established as shown in Fig. 9. Table 3 lists some of the important specifications of the vibration motors. Figure 10 shows a photograph of the hexahedral vibration motor that has been developed by the proposed design procedure. Since the cylinder type needs an additional fixture for the mounting, it can be said that the hexahedral type has the lowest volume and weight. It should be also noted that the hexahedral type can make use of any redundant space within a mobile phone since it can be mounted vertically as well as horizontally. Table 4 shows vibration test results for the given

Table 4 Test results of vibration motors

Mounting point	Coin type		Hexahedral type		Cylinder type		Measuring point
	RPM	Acc.(G)	RPM	Acc.(G)	RPM	Acc.(G)	
1	7380	0.659	11880	0.569	11580	0.015	A
2	7440	0.654	11640	0.537	11580	0.033	
3	7560	0.686	11640	0.536	11520	0.055	
4	—	—	11640	0.994	11820	0.856	

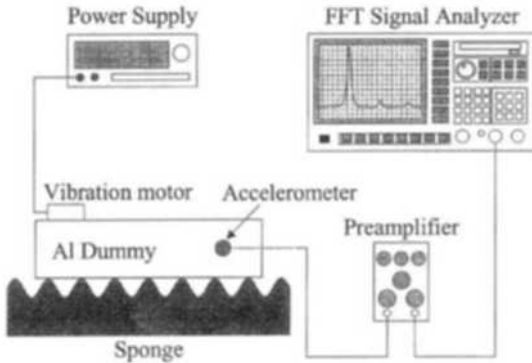


Fig. 9 Test setup for acceleration measurements

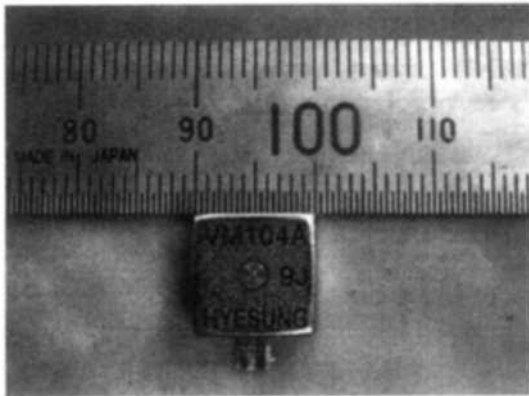


Fig. 10 Photograph of the hexahedral vibration motor

motors. With normal mounting points, the coin type shows the best performance. However, for the mounting point 4 that is available for the hexahedral type, it shows an excellent performance since it can effectively excite the dummy block. Noting that the hexahedral motor is more flexible for mounting due to its shape and volume, it can provide higher vibration once attached properly.

6. Conclusion

Vibration motor in mobile phones needs to be smaller and lighter to meet the recent trend of mobile phones. In this paper, a new hexahedral type vibration motor is developed using FEM analysis and genetic algorithm as an optimization technique. It practically has the lowest volume and weight compared to the conventional vibration motors. Due to the high flexibility of attachment for the hexahedral type, it can also provide sufficient vibration if it is attached properly.

References

Alhamadi, M. and Demerdash, N., 1994, "Three Dimensional Magnetic Field Computation by a Coupled Vector-Scalar Potential Method in Brushless DC Motors with Skewed Permanent Magnet Mounts—the-No-Load and Load Results," *IEEE Trans. Energy Conversion*, Vol. 9, No. 1, pp. 15~22.

Jang, G. H. and Lieu, D. K., 1996, "Analysis of the Magnetic Force and the Torque in a Brushless DC Motor," *KSME International Journal*, Vol. 10, No. 1, pp. 37~48.

Liu, Z. J., Bi, C., Tan, H.C. and Low, T-S., 1994, "Modeling and Torque Analysis of Permanent Magnet Spindle Motor for Disk Drive Systems," *IEEE Trans. Magnetics*, Vol. 30, No. 6, pp. 4317~4319.

Wurtz, F., Richomme, M., Bignon, J. and Sabonnadiere, C., 1997, "A Few Results for using Genetic Algorithms in the Design of Electrical Machines," *IEEE Transactions on Magnetics*, Vol. 33, No. 2, pp. 1892~1895.